



Polyanhydride nanovaccine against swine influenza virus in pigs



Santosh Dhakal^{a,b}, Jonathan Goodman^c, Kathryn Bondra^{a,b}, Yashavanth S. Lakshmanappa^{a,b}, Jagadish Hiremath^{a,b}, Duan-Liang Shyu^{a,b}, Kang Ouyang^{a,b}, Kyung-il Kang^{a,b}, Steven Krakowka^d, Michael J. Wannemuehler^e, Chang Won Lee^{a,b}, Balaji Narasimhan^c, Gourapura J. Renukaradhya^{a,b,*}

^a Food Animal Health Research Program, Ohio Agricultural Research and Development Center, 1680 Madison Avenue, Wooster, OH 44691, USA

^b Department of Veterinary Preventive Medicine, College of Veterinary Medicine, The Ohio State University, Columbus, OH 43210, USA

^c Department of Chemical and Biological Engineering, Iowa State University, Ames, IA 50011, USA

^d The Department of Veterinary Biosciences, College of Veterinary Medicine, The Ohio State University, 1925 Coffey Road, Columbus, OH, USA

^e Department of Veterinary Microbiology and Preventive Medicine, Iowa State University, Ames, IA, USA

ARTICLE INFO

Article history:

Received 21 November 2016

Received in revised form 9 January 2017

Accepted 12 January 2017

Available online 20 January 2017

Keywords:

Swine influenza virus

Polyanhydride nanoparticles

Intranasal

Immunity

Pigs

ABSTRACT

We have recently demonstrated the effectiveness of an influenza A virus (IAV) subunit vaccine based on biodegradable polyanhydride nanoparticles delivery in mice. In the present study, we evaluated the efficacy of ~200 nm polyanhydride nanoparticles encapsulating inactivated swine influenza A virus (SwIAV) as a vaccine to induce protective immunity against a heterologous IAV challenge in pigs. Nursery pigs were vaccinated intranasally twice with inactivated SwIAV H1N2 (KAg) or polyanhydride nanoparticle-encapsulated KAg (KAg nanovaccine), and efficacy was evaluated against a heterologous zoonotic virulent SwIAV H1N1 challenge. Pigs were monitored for fever daily. Local and systemic antibody responses, antigen-specific proliferation of peripheral blood mononuclear cells, gross and microscopic lung lesions, and virus load in the respiratory tract were compared among the groups of animals. Our pre-challenge results indicated that KAg nanovaccine induced virus-specific lymphocyte proliferation and increased the frequency of CD4⁺CD8 $\alpha\alpha$ ⁺ T helper and CD8⁺ cytotoxic T cells in peripheral blood mononuclear cells. KAg nanovaccine-immunized pigs were protected from fever following SwIAV challenge. In addition, pigs immunized with the KAg nanovaccine presented with lower viral antigens in lung sections and had 6 to 8-fold reduction in nasal shedding of SwIAV four days post-challenge compared to control animals. Immunologically, increased IFN- γ secreting T lymphocyte populations against both the vaccine and challenge viruses were detected in KAg nanovaccine-immunized pigs compared to the animals immunized with KAg alone. However, in the KAg nanovaccine-immunized pigs, hemagglutination inhibition, IgG and IgA antibody responses, and virus neutralization titers were comparable to that in the animals immunized with KAg alone. Overall, our data indicated that intranasal delivery of polyanhydride-based SwIAV nanovaccine augmented antigen-specific cellular immune response in pigs, with promise to induce cross-protective immunity.

© 2017 Elsevier Ltd. All rights reserved.

1. Introduction

Swine influenza A virus (SwIAV) causes considerable economic losses in the pig industry worldwide [1]. Currently, multiple antigenically diverse strains of three major SwIAV subtypes H1N1, H1N2 and H3N2 are circulating in pig populations. Since pigs serve as a mixing vessel for human and avian IAV, numerous distinct SwIAV strains are frequently generated, and some of these have

zoonotic potential [2]. An effective vaccination strategy can prevent economic losses in the pig industry and limit zoonotic transmission of SwIAVs to humans. Vaccination against SwIAV is frequently practiced on pig farms using either bivalent or multivalent whole virus inactivated (WIV) vaccines which protect against homologous virus but are ineffective against heterologous strains [3–6]. Since SwIAV undergoes frequent mutation with antigenic drift and shift, there is an urgent need to develop broadly cross-protective vaccines. Moreover, WIV vaccines do not elicit high levels of antigen-specific secretory IgA antibody response in the respiratory tract where the disease is localized. It is also known that strong mucosal immunity can correlate with cross-protective efficacy against influenza [7,8]. Recently, WIV vaccine

* Corresponding author at: Food Animal Health Research Program, Ohio Agricultural Research and Development Center, The Ohio State University, 1680 Madison Avenue, Wooster, OH 44691, USA.

E-mail address: gourapura.1@osu.edu (G.J. Renukaradhya).

formulations were reported to enhance the severity of lung lesions in pigs infected with heterologous IAV, raising concerns over judicious selection and use of vaccines [3,4,6]. To overcome these limitations, a novel vaccine delivery platform is needed for prevention and control of influenza in pigs.

Biodegradable and biocompatible polyanhydrides have been widely used for vaccine antigen delivery due to safety [9–11] and their adjuvant properties [12]. The most well-studied polyanhydride copolymers are based on sebacic acid (SA), 1,6-bis(*p*-carboxyphenoxy)hexane (CPH), and 1,8-bis(*p*-carboxyphenoxy)-3,6-dioxatane (CPTEG) monomers. Polyanhydrides are surface eroding polymers, which minimize the exposure of encapsulated antigen to moisture providing a better microenvironment for the encapsulated vaccine antigen(s) [12,13]. Polyanhydride nanoparticles retain the structural and biological activity of released vaccine antigens [14–19] and also have pathogen mimicking properties to activate dendritic cells and enhance innate immune response [19–22]. Recent studies have shown induction of high virus neutralizing antibody titer and enhanced cell-mediated immune responses against IAV in mice vaccinated with a hemagglutinin-based polyanhydride nanovaccine [23,24]. In this study, we analyzed the immunogenicity and protective efficacy of 20:80 CPTEG:CPH nanoparticles encapsulating whole inactivated SwIAV vaccine against a heterologous and virulent zoonotic SwIAV H1N1 challenge in pigs. Our results indicated that nanovaccine encapsulation of SwIAV augmented the virus specific cell-mediated immune response and reduced the virus load and fever in pigs.

2. Materials and methods

2.1. Vaccine preparation

The SwIAV isolates, SW/OH/FAH10-1/10 H1N2 a δ lineage virus bearing human like HA and NA genes, swine triple reassortant virus internal genes PB2, PB1, PA and NS and pandemic H1N1 lineage NP and M genes [25], and SW/OH/24366/2007 H1N1 a triple reassortant γ lineage virus having swine origin HA, NA, NP, M and NS genes, human origin PB1 and avian origin PB2 and PA genes [26] were used in vaccine preparation and challenge infection, respectively.

For vaccine preparation, Madin-Darby canine kidney (MDCK) cell grown H1N2 virus culture fluid was concentrated by sucrose gradient ultra-centrifugation, and the virus was inactivated by binary ethyleneimine (BEI). Inactivated/killed SwIAV (KAg) was encapsulated in 20:80 CPTEG:CPH polyanhydride nanoparticles (KAg nanovaccine) as described previously [27,28]. Particle size and morphology were examined by a FEI Quanta 250 scanning electron microscope (SEM, Kyoto, Japan) and size distribution was characterized by using ImageJ software with an average of 200 nanoparticles and with quasi-elastic light scattering experiments (QELS) using a Zetasizer Nano (Malvern Instruments Ltd., Worcester, UK). The SwIAV encapsulation efficiency in the nanoparticles was determined as described previously [14].

2.2. Experimental design and sample collection

Caesarian-delivered colostrum-deprived (CDCD) and bovine colostrum-fed Large White-Duroc crossbred piglets ($n = 30$) were raised in the BSL2 facility at OARDC as described previously [29]. Piglets were confirmed seronegative for hemagglutination inhibition (HI) antibodies against SwIAV H1N1 and H1N2, and were randomly divided into 4 experimental groups ($n = 7$ or 8 pigs/group) (Table 1). Maintenance of pigs and all experimental procedures were conducted in accordance with the guidelines of the

Institutional Animal Care and Use Committee at The Ohio State University.

Animals were vaccinated at 4–5 weeks, boosted after 3 weeks, and challenged after 2 weeks of boost i.e., day post-vaccination (DPV) 35. For each vaccination dose, pigs intranasally received 10^7 TCID₅₀ equivalent of inactivated H1N2 virions (KAg) or KAg entrapped within the nanoparticles (KAg nanovaccine) suspended in 2 mL DMEM. The challenge SwIAV inoculum consisted of a virulent, zoonotic, and heterologous SwIAV H1N1 (6×10^6 TCID₅₀ in 2 mL) of which 1 mL was administered intranasally and 1 mL intratracheally [26]. Plasma samples were collected at the time of vaccination and necropsy. After challenge the rectal temperature was recorded daily, and nasal swab samples were collected in 2 mL of DMEM at four days post-challenge (DPC). Pigs were euthanized at six DPC and lungs were examined and scored for gross lesions [30]. Broncho-alveolar lavage (BAL) fluid was collected for virus titration and lung lysate (prepared using 1 g of tissue from the right apical lobe suspended in 3 mL of DMEM, which was homogenized and the supernatant was collected) was analyzed for antibody response [31]. Lung tissues were formalin fixed for histopathological and immunohistochemical evaluations. PBMCs were isolated by using density gradient medium Lymphoprep in SepMate-50 tubes (Stemcell, BC, Canada) as per the manufacturer's instructions at DPC 0 and 6 for lymphocyte proliferation and flow cytometry assays.

2.3. Cell proliferation and flow cytometry assays

SwIAV antigen-specific lymphocyte proliferation was assessed using PBMCs and the cell titer 96 aqueous non-radioactive proliferation assay kit (Promega, WI) as per the manufacturer's instructions. One million cells per well were seeded in triplicates in 96 well sterile U-bottom plate (Greiner bio-one, NC) and stimulated with live SwIAV H1N2 at 0.1 MOI or with medium control. After 72 h of incubation at 37 °C in a 5% CO₂ incubator, MTS + PMS solution was added and the OD_{490nm} was measured after 4 h using an ELISA plate reader (Spectramax Plus384, Molecular Devices, CA). Stimulation index (SI) was determined by dividing OD of stimulated PBMCs by OD of cell control of the same pig.

PBMCs isolated at DPC 0 were also analyzed to determine the frequency of different T cell subsets by flow cytometry. At DPC 6, isolated PBMCs were stimulated with live SwIAV H1N2 or H1N1 at MOI 0.1 for 72 h, and cells were immunostained and analyzed by flow cytometry to determine the frequency of activated (IFN- γ^+) T cell subsets as described previously [29]. Antibodies used in the assay were anti-porcine CD3 ϵ , CD4 α and CD8 α (Southernbiotech, AL), CD8 β , δ -chain, and IFN γ (BD biosciences, CA) along with their respective isotype controls.

2.4. Virus titration

Serial tenfold dilutions of BAL fluid and nasal swabs were prepared in DMEM supplemented with TPCK-trypsin (1 μ g/mL) and transferred to MDCK cells grown on 96 well cell culture plates. After 48 h of incubation at 37 °C in a 5% CO₂ incubator, cells were immunostained using IAV nucleoprotein specific primary antibody (#M058, CalBioagents, CA) followed by AlexaFluor 488 conjugated goat anti-mouse IgG (H + L) antibody (Life technologies, OR). Immunofluorescence was recorded using fluorescent microscope (Olympus, NY) and infectious virus titer was calculated using the Reed and Muench method [29,32].

2.5. Antibody titration

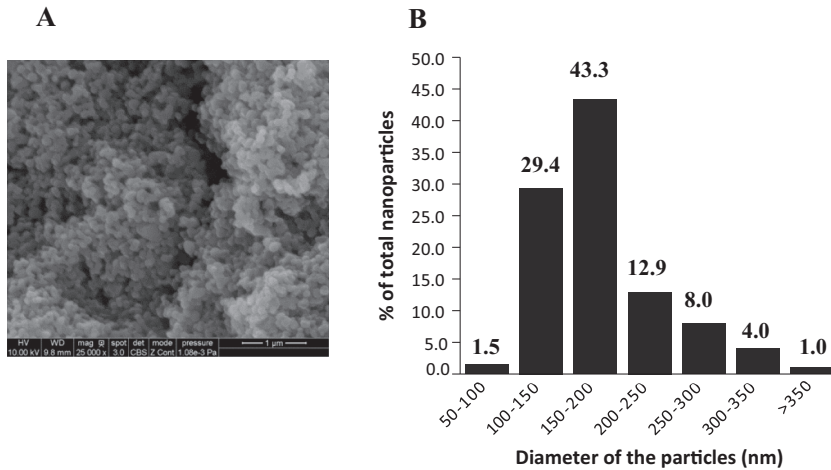
Hemagglutination inhibition (HI) titer and SwIAV-specific antibody responses were determined as described previously [29].

Table 1

Experimental design showing assignment of pigs in each group (n = number of pigs).

Experimental groups	n	Vaccine formulations		
		First vaccination (DPV 0/DPC -35)	Second vaccination (DPV 21/DPC -14)	Day of Challenge (DPV 35/DPC 0)
Mock	7	Mock inoculum	Mock inoculum	Mock inoculum
Mock + Ch.	8	Mock inoculum	Mock inoculum	SwIAV OH7 (H1N1)
KAg + Ch.	8	Inactivated SwIAV (H1N2)	Inactivated SwIAV (H1N2)	SwIAV OH7 (H1N1)
KAg Nanovaccine + Ch.	7	Inactivated SwIAV Nanovaccine (H1N2)	Inactivated SwIAV Nanovaccine (H1N2)	SwIAV OH7 (H1N1)

DPV - Day post-vaccination; DPC - Day post-challenge; Ch - SwIAV OH7 (H1N1) Challenge.

**Fig. 1.** Physical characterization of polyanhydride nanoparticles. (A) Surface morphology of KAg nanovaccine nanoparticles depicted by scanning electron photomicrograph (25Kx magnification). (B) Size distribution of KAg nanovaccine nanoparticles presented as percentage of total particles.

Undiluted nasal swab samples and 1:200 dilutions of BAL fluid, plasma and lung lysates were used in IgG and IgA antibody response comparison among the pig groups. Virus neutralization titer (VNT) in BAL fluid was also determined using procedures described previously [29].

2.6. Histopathology and Immunohistochemistry (IHC) analyses

Five micron sections of apical, cardiac and diaphragmatic lung lobes of pigs were stained with hematoxylin and eosin (H&E) and examined microscopically for histopathological changes as described previously [30]. Briefly, lesion severity was scored by the distribution or by the extent of lesions within the sections and PMN infiltration and graded 0 to 3. SwIAV-specific antigen in the lungs was detected by IHC as described previously [33,34] with a few modifications. SwIAV nucleoprotein specific antibody (#M058, CalBioReagents, CA) was used for immunostaining the viral antigens followed by treatment with VECTASTAIN elite ABC reagent (#PK-7100, Vector Labs, CA) to develop positive signal as per manufacturer's instructions. The reactivity of viral antigenic mass in the airway epithelial cells was evaluated in IHC analysis.

2.7. Statistical analysis

Data are presented and compared as median and range of 7 or 8 pigs in different groups. HI and VN titers are presented as geometric mean \pm 95% CI. Virus titers were log transformed and analyzed [34]. Non-parametric Kruskal-Wallis test followed by Dunn's post hoc test was used to compare the data in GraphPad Prism 5 (GraphPad Software, Inc., CA) considering a $P < 0.05$ as statistically significant.

3. Results

3.1. Physical characteristics of SwIAV nanovaccine

The morphology of the synthesized polyanhydride nanoparticles was spherical and the size of the majority of particles was between 100 and 200 nm as determined by scanning electron photomicrographs (Fig. 1A and B). The mean diameter of the antigen loaded nanoparticles as determined by ImageJ software (and confirmed with light scattering) was 181 ± 56 nm (Fig. 1B) [27,28]. The encapsulation efficiency of SwIAV H1N2 antigens within the nanoparticles was determined to be 60%.

3.2. Pre-challenge cellular and humoral immune responses in pigs

PBMCs isolated from vaccinated pigs at DPV 35/DPC 0 were stimulated with the vaccine virus (SwIAV H1N2) and lymphocyte proliferation was assessed. Our data suggested that lymphocyte stimulation index in KAg nanovaccine vaccinated pigs was significantly higher compared to that in the animals vaccinated with the KAg alone (Fig. 2A). KAg nanovaccine-immunized pigs but not the KAg alone vaccinated pigs had significantly higher frequency of T helper/memory cells ($CD3^+CD4^+CD8\alpha\alpha^+$) (Fig. 2B) and cytotoxic T lymphocytes (CTLs) ($CD3^+CD4^-CD8\alpha\beta^+$) compared to the mock group (Fig. 2C). The HI titer in plasma at DPC 0 was significantly higher against the vaccine virus in both KAg nanovaccine- and KAg-immunized pigs compared to mock controls, but no significant differences were observed between two vaccine groups (Fig. 2D). The IgG antibody response to the homologous vaccine virus in plasma at DPC 0 was also similar between KAg- and KAg nanovaccine-immunized animals (Fig. 2E) and the antibody

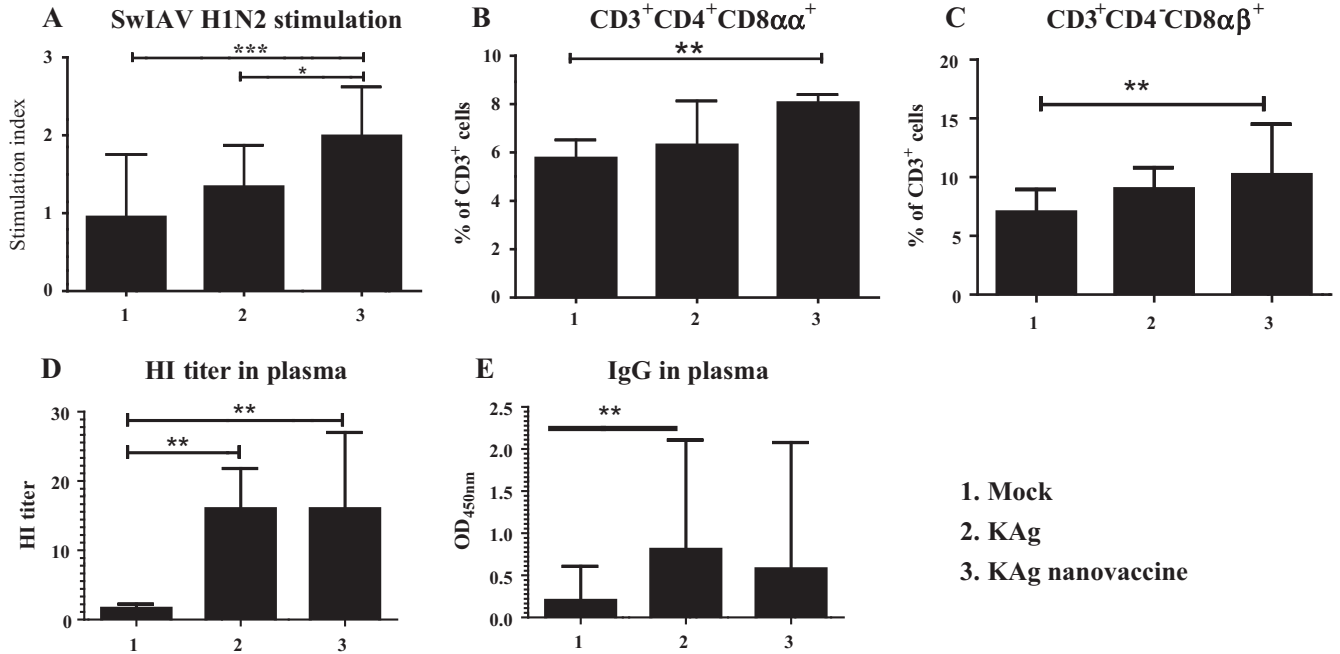


Fig. 2. Cellular and humoral immune responses in vaccinated pigs pre-challenge. (A) PBMCs isolated at DPV 35/DPC 0 were stimulated with vaccine virus (SwIAV H1N2) and lymphocyte proliferation was determined. PBMCs isolated at DPV 35/DPC 0 were also immunostained for phenotyping: (B) CD3⁺CD4⁺CD8αα⁺ (T helper/memory) and (C) CD3⁺CD4⁻CD8αβ⁺ (CTLs). For humoral immune response analyses: (D) HI titer and (E) total IgG antibody responses were determined as described in Methods. Each bar is the median and range value of 7 or 8 pigs. Panel D shows geometric mean ± 95% CI. Data were analyzed by non-parametric Kruskal-Wallis test followed by Dunn's post hoc test. Asterisk refers to statistical difference between two indicated pig groups (*p < 0.05; **p < 0.01 and ***p < 0.001).

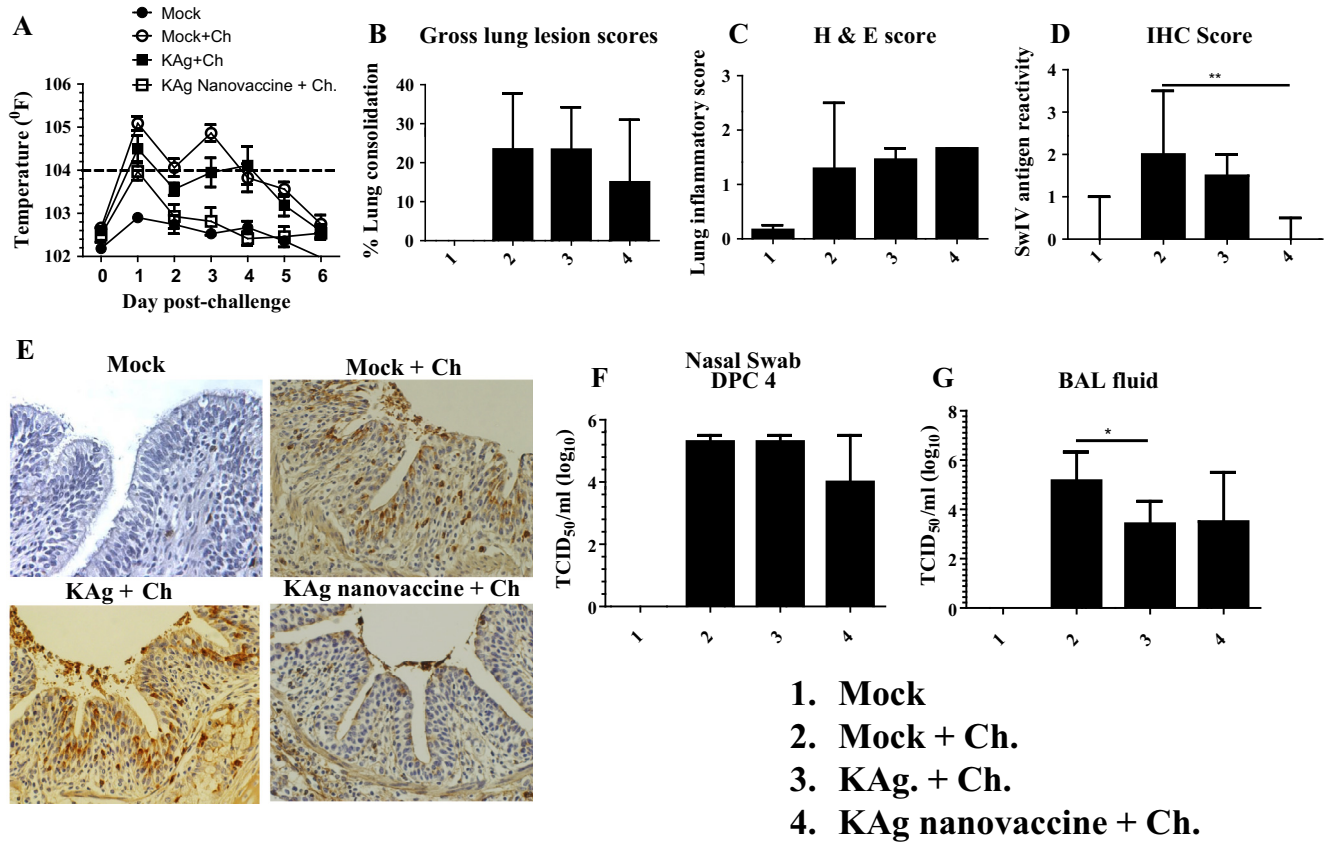


Fig. 3. Clinical and pathological changes and SwIAV H1N1 titration in vaccinated pigs post-challenge. (A) Graphs showing the average rectal body temperature recorded daily post-challenge; (B) gross lung lesions in pigs recorded during necropsy at DPC 6; (C) microscopic lung lesions scores of H&E stained lung sections; (D) immunohistochemistry analysis of lung sections for SwIAV antigens; and (E) representative pictures of lung sections of pigs analyzed for SwIAV antigens by Immunohistochemistry. Virus titers in (F) nasal swabs at DPC 4 and in (G) BAL fluid at DPC 6 are shown. The dashed line at temperature 104 °C indicates fever in pigs. Each bar is the median and range value of 7 or 8 pigs. Data were analyzed by non-parametric Kruskal-Wallis test followed by Dunn's post hoc test. Asterisk refers to statistical difference between two indicated pig groups (*p < 0.05 and **p < 0.01).

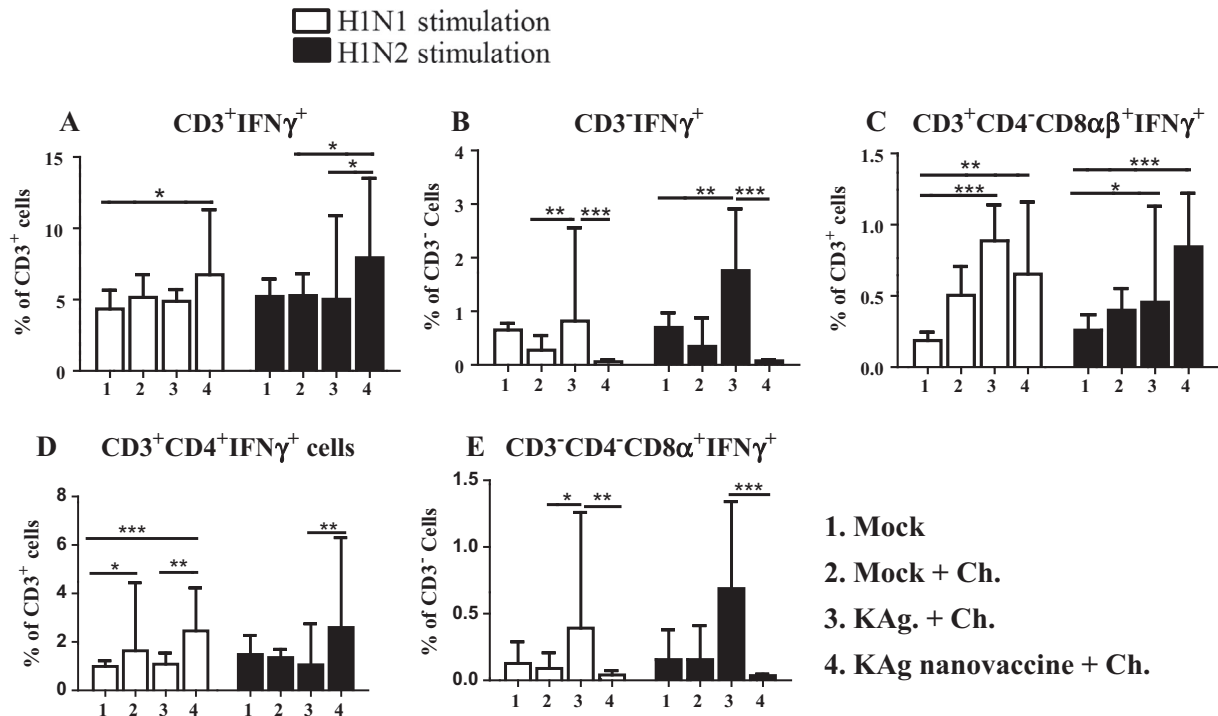


Fig. 4. Immunophenotyping of activated ($IFN\gamma^+$) lymphocytes in PBMCs of vaccinated pigs restimulated with the vaccine (H1N2) or challenge (H1N1) SwIAV *ex vivo*. Frequencies of (A) $CD3^+IFN\gamma^+$ (T cells); (B) $CD3^-IFN\gamma^+$ cells (non-T cells); (C) $CD3^+CD4^-CD8\alpha\beta^+IFN\gamma^+$ (CTLs); (D) $CD3^+CD4^+IFN\gamma^+$ (T-helper cells); and (E) $CD3^-CD4^-CD8\alpha^+IFN\gamma^+$ (NK cells) are shown. Each bar is the median and range value of 7 or 8 pigs. Data were analyzed by non-parametric Kruskal-Wallis test followed by Dunn's post hoc test. Asterisk refers to statistical difference between two indicated pig groups (* $p < 0.05$; ** $p < 0.01$ and *** $p < 0.001$).

response against the challenge heterologous virus was weak (data not shown).

3.3. Clinical and pathological changes and virus load post-challenge

The comparative protective efficacy of KAg nanovaccine vs. KAg alone was assessed in heterologous virus-challenged pigs. A body temperature of $104^\circ F$ is accepted as fever in pigs [35]. Mock-challenged and KAg-vaccinated pigs had fever at DPC 1 to 4, while KAg nanovaccine-immunized pigs had fever only at DPC 1 (Fig. 3A). Though not statistically significant, the gross lesions involved a smaller area of the lungs in KAg nanovaccine-immunized animals compared to the animals vaccinated with KAg (Fig. 3B). The H&E scores at DPC 6 were comparable among all three groups of virus challenged pigs (Fig. 3C). The mean IHC scores for SwIAV antigen reactivity in the lung sections was significantly reduced in KAg nanovaccine-immunized animals compared to the mock vaccinated and virus challenged pigs, but not in KAg alone vaccinated group (Fig. 3D); representative lung pictures of bronchial epithelial cells with virus antigens is shown (Fig. 3E).

Consistent with the lung IHC scores, the nasal virus shedding at DPC 4 in KAg nanovaccine group was six- and eightfold lower than KAg and mock vaccinated and SwIAV H1N1 challenged groups, respectively (Fig. 3F). However, at DPC 6 the challenge virus titer in BAL fluid was reduced in both KAg (40-fold) and KAg nanovaccine-immunized (37-fold) pig groups compared to mock vaccinated and virus challenged pigs (Fig. 3G), suggesting less replication/shedding in the airway epithelium of the vaccinated pigs.

3.4. Activated recall $IFN\gamma$ secreting lymphocyte response in the blood post-challenge

To assess the recall cellular immune response post-challenge, isolated PBMCs were stimulated with vaccine (H1N2) and chal-

lenge (H1N1) SwIAV virions to estimate the frequencies of activated (i.e., $IFN\gamma^+$) lymphocyte subsets. The frequency of activated T cells ($CD3^+IFN\gamma^+$) (Fig. 4A) and T helper cells ($CD3^+CD4^+IFN\gamma^+$) (Fig. 4D) were significantly higher in animals vaccinated with KAg nanovaccine stimulated with both the H1N1 and H1N2 viruses compared to that in animals vaccinated with KAg alone. The frequency of activated CTLs ($CD3^+CD4^-CD8\alpha\beta^+IFN\gamma^+$) were significantly higher in both KAg nanovaccine and KAg vaccinated pig groups stimulated with both the H1N1 and H1N2 viruses compared to mock control pig group (Fig. 4C). The innate $CD3^-IFN\gamma^+$ non-T cells (Fig. 4B) as well as $CD3^-CD4^-CD8\alpha^+IFN\gamma^+$ NK cells (Fig. 4E) were found to be significantly higher in KAg- compared to KAg nanovaccine-immunized animals.

3.5. Humoral immune response post-challenge

In post-challenged pigs, the specific antibody response against the challenge virus was analyzed both locally and systemically (Fig. 5). The virus-specific IgA antibody response in nasal swabs (Fig. 5A), BAL fluid (Fig. 5B), and lung lysates (Fig. 5C) were significantly higher in KAg (but not KAg nanovaccine) vaccinated compared to both mock control and mock challenge pig groups; while the IgA levels between the KAg and KAg nanovaccine-immunized pig groups was not statistically different. Specific IgG response in plasma (Fig. 5D) and BAL fluid (Fig. 5E), HI titers in BAL fluid (Fig. 5F) and plasma (Fig. 5G), and VN titers in BAL fluid (Fig. 5H) were comparable in the animals immunized with KAg and KAg nanovaccine.

4. Discussion

Induction of protective immunity against influenza is possible under field conditions only by developing a vaccine that elicits robust immune responses against conserved viral antigens, but

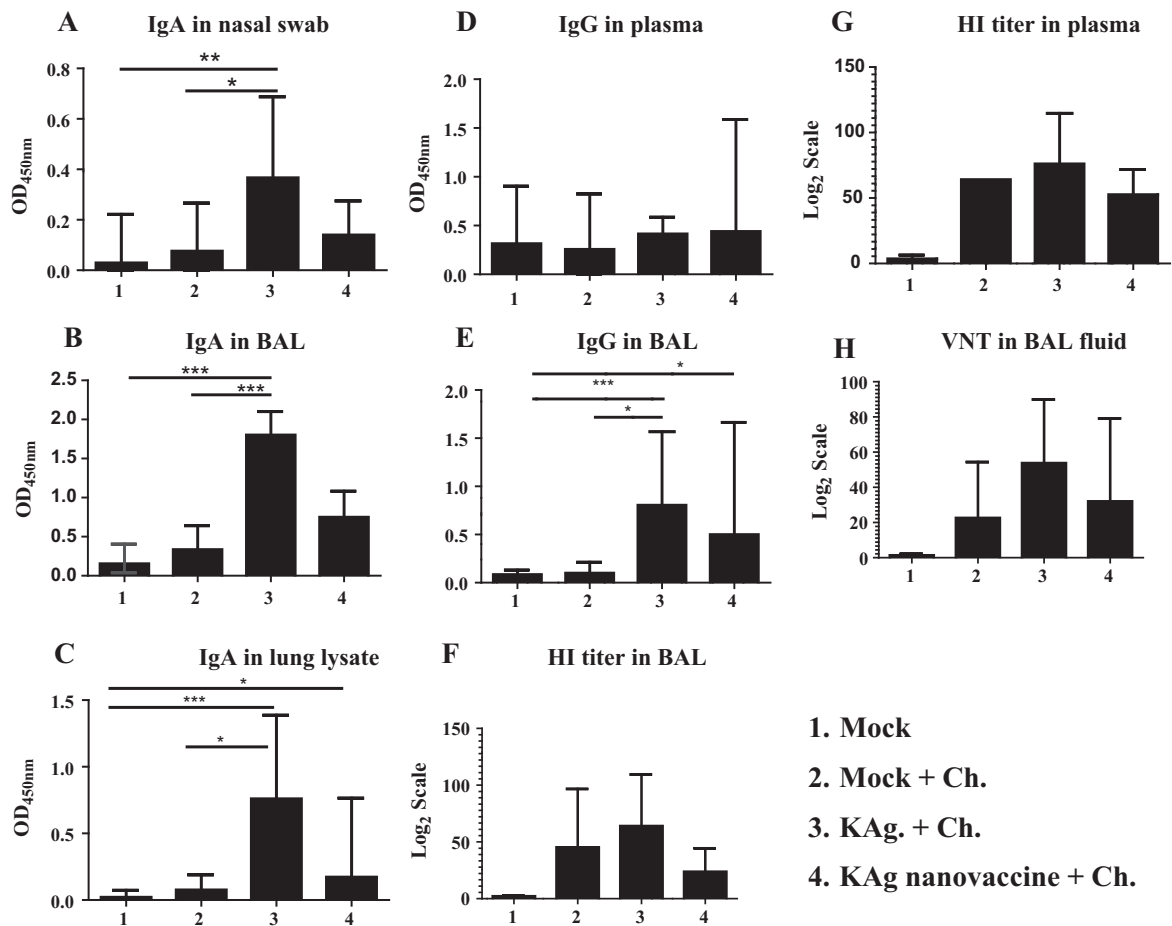


Fig. 5. Humoral immune response in vaccinated pigs post-challenge against the challenge virus. Antibody analysis was performed by ELISA to determine the levels of humoral response: IgA in (A) nasal swab; (B) BAL fluid; (C) lung lysate; and IgG response in (D) plasma and (E) BAL fluid. SwIAV H1N2 specific titers of HI antibodies in (F) BAL fluid and (G) plasma; and (H) VN titers in BAL fluid were determined. Each bar is the median and range value of 7 or 8 pigs. Panels F, G, H show geometric mean \pm 95% CI. Data were analyzed by non-parametric Kruskal-Wallis test followed by Dunn's post hoc test. Asterisk refers to statistical difference between two indicated pig groups ($p < 0.05$; $**p < 0.01$ and $***p < 0.001$).

current SwIAV vaccines have failed to do that. To achieve that goal, we evaluated the immunogenicity and cross-protective efficacy of a polyanhydride-based nanoparticle encapsulated killed SwIAV vaccine administered intranasally in influenza antibody-free pigs. The KAg nanovaccine rescued pigs from heterologous virulent SwIAV induced clinical symptoms and fever, associated with reduced gross lung pathology, slightly reduced nasal virus shedding and antigenic load in the lungs. This is likely mediated by the induction of robust antigen-specific cell-mediated immune responses against the challenge virus, in spite of the lack of induction of an enhanced antibody response. The lack of an enhanced antibody response in the KAg nanovaccine-immunized animals may be attributed to little to no disease being observed in those animals with only modest viral replication in the lungs. These observations would point to an absence of an anamnestic antibody response, which merits further investigation.

Polyanhydride micro/nanoparticles based on CPTEG, CPH and SA have been widely studied for vaccine and drug delivery against viral, bacterial and parasitic pathogens in rodent models [36]. In this work, we used the 20:80 CPTEG:CPH-based nanoparticle formulation because it has been shown to be a potent adjuvant based on its ability to enhance both humoral and cellular immune responses to vaccine antigens [12,27,28,37]. Amphiphilic polyanhydrides based on CPTEG and CPH facilitate slow release of antigen, conserve protein structure and stability, and maintain immunogenicity of the antigenic epitopes [17]. Polyanhydride

nanovaccines have also induced antigen-specific memory T cells and profound recall responses in mice [38,39]. A previous study involving 20:80 CPTEG:CPH-based nanoparticle encapsulated recombinant H5 trimer vaccine against H5N1 influenza challenge in mice enhanced the CD4⁺ T cell recall response and showed protective efficacy [23]. Consistent with these findings, the current study in pigs with intranasal immunization with KAg nanovaccine induced a strong cell-mediated immune response by enhancing the antigen specific lymphocyte proliferation and increasing the frequency of T helper/memory cells and CTLs. Furthermore, in post-challenged pigs, the IFN- γ producing T cell sub-population was increased in *ex vivo* cultures of PBMCs stimulated with antigens from both vaccine and challenge viruses.

In addition, it is important to use low doses of antigens in vaccine formulations in order to prevent unwanted side effects. Polyanhydride nanovaccines have been reported to induce strong antibody response along with dose-sparing capabilities. For example, a suboptimal dose of ovalbumin (25 μ g) in polyanhydride particles delivered subcutaneously in mice induced antibody response similar to that induced by delivering 400–1600 μ g of the soluble antigen [40]. A 20:80 CPTEG:CPH particle-based formulation containing 20 μ g hemagglutinin protein of H5N1 virus was also shown to induce robust VN titer in a homologous challenge trial in mice [23]. In the current study in pigs the 20:80 CPTEG:CPH polyanhydride nanoparticle-encapsulated SwIAV KAg induced similar systemic and local antigen-specific VN and HI antibody titers

compared to pigs immunized with the KAg alone. Intranasal vaccination of mice has been shown to induce better mucosal IgA responses compared to parenteral immunization. In mice, intranasal delivery of 50:50 CPTEG:CPH polyanhydride based vaccine showed protective efficacy against *Yersinia pestis* challenge mediated mainly by a high titer antibody response [41]. In contrast to mice, it appears that intranasal administration of the 20:80 CPTEG:CPH polyanhydride nanovaccine formulation induces more of a cellular than a humoral immune response in pigs.

The size, charge, and other characteristics of nanoparticles play a major role on favorable outcome of vaccination. Particle size of less than or equal to 500 nm is considered suitable to be taken up readily by APCs [42,43]. In mice, 360–470 nm particles were found to be suitable for adequate pulmonary distribution [44]. Thus, our 100–300 nm polyanhydride nanoparticles were of appropriate size for intranasal vaccine delivery in pigs. We detected low and comparable titers of the challenge virus in the BAL fluid of pigs that received KAg nanovaccine and soluble vaccine antigen at DPC 6. This indicates that, despite the benefit of improved cellular immunity, there is a need to improve the efficacy of polyanhydride nanoparticle-based vaccine delivery platform in pigs for induction of better cross-protection.

The controlled release of antigen, pathogen mimicking properties and in vivo immune modulation capabilities of polyanhydride nanoparticles are dependent on polymer chemistry [17,28,37,45]. Hence, the polymer formulation and route of delivery best suited in one animal model may or may not be suitable in other animal model or species. Our preliminary findings suggest that there was no adverse effect of intranasal administration of 20:80 CPTEG:CPH polyanhydride nanoparticles in pigs. Furthermore, this vaccine delivery platform provided clinical protection against a virulent heterologous virus challenge by inducing robust antigen-specific cell-mediated immune response, in spite of not inducing enhanced antibody response, indicating the immunological benefits of the nanovaccine in pigs. Our future studies will be focused on optimizing the nanoparticle chemistry and vaccine formulation so as to exploit the inherent adjuvant properties of polyanhydride nanoparticles aimed to further enhance the cross-protective efficacy of SwIAV vaccines in pigs.

Acknowledgements

We are thankful to Dr. Juliette Hanson and Megan Strother who provided help in animal studies, and Kathleen Ross (Iowa State University) for statistical help. This work was supported by Nanovaccine Initiative, Iowa State University and Agriculture and Food Research Initiative Competitive Grant no. 2013-67015-20476 from the USDA-NIFA. Salaries and research support were provided by state and federal funds appropriated to OARDC, The Ohio State University.

References

- [1] Dykhuus HC, Painter T, Fangman T, Holtkamp D. Assessing production parameters and economic impact of swine influenza, PRRS and Mycoplasma hyopneumoniae on finishing pigs in a large production system. In: Proceedings of AASV annual meeting; 2012. p. 75–6.
- [2] Vincent A, Awada L, Brown I, Chen H, Claes F, Dauphin G, et al. Review of influenza A virus in swine worldwide: a call for increased surveillance and research. *Zoonoses Public Health* 2014;61:4–17.
- [3] Gauger PC, Vincent AL, Loving CL, Lager KM, Janke BH, Kehrl Jr ME, et al. Enhanced pneumonia and disease in pigs vaccinated with an inactivated human-like (delta-cluster) H1N2 vaccine and challenged with pandemic 2009 H1N1 influenza virus. *Vaccine* 2011;29:2712–9.
- [4] Vincent AL, Lager KM, Janke BH, Gramer MR, Richt JA. Failure of protection and enhanced pneumonia with a US H1N2 swine influenza virus in pigs vaccinated with an inactivated classical swine H1N1 vaccine. *Vet Microbiol* 2008;126:310–23.
- [5] Vincent AL, Ciacci-Zanella JR, Lorusso A, Gauger PC, Zanella EL, Kehrl Jr ME, et al. Efficacy of inactivated swine influenza virus vaccines against the 2009 A/H1N1 influenza virus in pigs. *Vaccine* 2010;28:2782–7.
- [6] Kitikoon P, Vincent AL, Janke BH, Erickson B, Strait EL, Yu S, et al. Swine influenza matrix 2 (M2) protein contributes to protection against infection with different H1 swine influenza virus (SIV) isolates. *Vaccine* 2009;28:523–31.
- [7] Tamura S, Kurata T. Defense mechanisms against influenza virus infection in the respiratory tract mucosa. *Jpn J Infect Dis* 2004;57:236–47.
- [8] van Riet E, Ainai A, Suzuki T, Hasegawa H. Mucosal IgA responses in influenza virus infections; thoughts for vaccine design. *Vaccine* 2012;30:5893–900.
- [9] Vela-Ramirez JE, Goodman JT, Boggiatto PM, Roychoudhury R, Pohl NL, Hostetter JM, et al. Safety and biocompatibility of carbohydrate-functionalized polyanhydride nanoparticles. *AAPS J* 2015;17:256–67.
- [10] Huntimer L, Ramer-Tait AE, Petersen LK, Ross KA, Walz KA, Wang C, et al. Evaluation of biocompatibility and administration site reactivity of polyanhydride-particle-based platform for vaccine delivery. *Adv Healthcare Mater* 2013;2:369–78.
- [11] Adler AF, Petersen LK, Wilson JH, Torres MP, Thorstenson JB, Gardner SW, et al. High throughput cell-based screening of biodegradable polyanhydride libraries. *Comb Chem High Throughput Screening* 2009;12:634–45.
- [12] Mallapragada SK, Narasimhan B. Immunomodulatory biomaterials. *Int J Pharm* 2008;364:265–71.
- [13] Determan AS, Trewyn BG, Lin VS, Nilsen-Hamilton M, Narasimhan B. Encapsulation, stabilization, and release of BSA-FITC from polyanhydride microspheres. *J Control Release* 2004;100:97–109.
- [14] Ross KA, Loyd H, Wu W, Huntimer L, Wannemuehler MJ, Carpenter S, et al. Structural and antigenic stability of H5N1 hemagglutinin trimer upon release from polyanhydride nanoparticles. *J Biomed Mater Res A* 2014;102:4161–8.
- [15] Vela Ramirez JE, Roychoudhury R, Habte HH, Cho MW, Pohl NL, Narasimhan B. Carbohydrate-functionalized nanovaccines preserve HIV-1 antigen stability and activate antigen presenting cells. *J Biomater Sci Polym Ed* 2014;25:1387–406.
- [16] Haughney SL, Petersen LK, Schoofs AD, Ramer-Tait AE, King JD, Briles DE, et al. Retention of structure, antigenicity, and biological function of pneumococcal surface protein A (PspA) released from polyanhydride nanoparticles. *Acta Biomater* 2013;9:8262–71.
- [17] Lopac SK, Torres MP, Wilson-Welder JH, Wannemuehler MJ, Narasimhan B. Effect of polymer chemistry and fabrication method on protein release and stability from polyanhydride microspheres. *J Biomed Mater Res B Appl Biomater* 2009;91:938–47.
- [18] Carrillo-Conde B, Schiltz E, Yu J, Chris Minion F, Phillips GJ, Wannemuehler MJ, et al. Encapsulation into amphiphilic polyanhydride microparticles stabilizes *Yersinia pestis* antigens. *Acta Biomater* 2010;6:3110–9.
- [19] Torres MP, Determan AS, Anderson GL, Mallapragada SK, Narasimhan B. Amphiphilic polyanhydrides for protein stabilization and release. *Biomaterials* 2007;28:108–16.
- [20] Phanse Y, Carrillo-Conde BR, Ramer-Tait AE, Roychoudhury R, Pohl NL, Narasimhan B, et al. Functionalization of polyanhydride microparticles with di-mannose influences uptake by and intracellular fate within dendritic cells. *Acta Biomater* 2013;9:8902–9.
- [21] Petersen LK, Ramer-Tait AE, Broderick SR, Kong CS, Ulerly BD, Rajan K, et al. Activation of innate immune responses in a pathogen-mimicking manner by amphiphilic polyanhydride nanoparticle adjuvants. *Biomaterials* 2011;32:6815–22.
- [22] Carrillo-Conde B, Song EH, Chavez-Santoscoy A, Phanse Y, Ramer-Tait AE, Pohl NL, et al. Mannose-functionalized “pathogen-like” polyanhydride nanoparticles target C-type lectin receptors on dendritic cells. *Mol Pharm* 2011;8:1877–86.
- [23] Ross KA, Loyd H, Wu W, Huntimer L, Ahmed S, Sambol A, et al. Hemagglutinin-based polyanhydride nanovaccines against H5N1 influenza elicit protective virus neutralizing titers and cell-mediated immunity. *Int J Nanomed* 2015;10:229–43.
- [24] Ross KA, Adams JR, Loyd H, Ahmed S, Sambol A, Broderick SR, et al. Combination nanovaccine demonstrates synergistic enhancement in efficacy against influenza. *ACS Biomater Sci Eng* 2016;2:368–74.
- [25] Ali A, Khatri M, Wang L, Saif YM, Lee CW. Identification of swine H1N2/pandemic H1N1 reassortant influenza virus in pigs, United States. *Vet Microbiol* 2012;158:60–8.
- [26] Yassine HM, Khatri M, Zhang YJ, Lee CW, Byrum BA, O’Quin J, et al. Characterization of triple reassortant H1N1 influenza A viruses from swine in Ohio. *Vet Microbiol* 2009;139:132–9.
- [27] Binnebose AM, Haughney SL, Martin R, Imerman PM, Narasimhan B, Bellaire BH. Polyanhydride nanoparticle delivery platform dramatically enhances killing of filarial worms. *PLoS Negl Trop Dis* 2015;9:e0004173.
- [28] Goodman JT, Vela Ramirez JE, Boggiatto PM, Roychoudhury R, Pohl NLB, Wannemuehler MJ, et al. Nanoparticle chemistry and functionalization differentially regulates dendritic cell-nanoparticle interactions and triggers dendritic cell maturation. *Part Part Syst Charact* 2014;31:1269–80.
- [29] Hiremath J, Kang KI, Xia M, Elaihs M, Binjawadagi B, Ouyang K, et al. Entrapment of H1N1 influenza virus derived conserved peptides in PLGA nanoparticles enhances T cell response and vaccine efficacy in pigs. *PLoS ONE* 2016;11:e0151922.
- [30] Khatri M, Dwivedi V, Krakowka S, Manickam C, Ali A, Wang L, et al. Swine influenza H1N1 virus induces acute inflammatory immune responses in pig lungs: a potential animal model for human H1N1 influenza virus. *J Virol* 2010;84:11210–8.

- [31] Renukaradhya GJ, Alekseev K, Jung K, Fang Y, Saif LJ. Porcine reproductive and respiratory syndrome virus-induced immunosuppression exacerbates the inflammatory response to porcine respiratory coronavirus in pigs. *Viral Immunol* 2010;23:457–66.
- [32] Reed LJ, Muench L. A simple method of estimating fifty per cent endpoints. *Am J Hygiene* 1938;27(3):493–7.
- [33] Dwivedi V, Manickam C, Binjawadagi B, Joyappa D, Renukaradhya GJ. Biodegradable nanoparticle-entrapped vaccine induces cross-protective immune response against a virulent heterologous respiratory viral infection in pigs. *PLoS ONE* 2012;7:e51794.
- [34] Richt JA, Lekcharoensuk P, Lager KM, Vincent AL, Loiacono CM, Janke BH, et al. Vaccination of pigs against swine influenza viruses by using an NS1-truncated modified live-virus vaccine. *J Virol* 2006;80:11009–18.
- [35] Risatti GR, Callahan JD, Nelson WM, Borca MV. Rapid detection of classical swine fever virus by a portable real-time reverse transcriptase PCR assay. *J Clin Microbiol* 2003;41:500–5.
- [36] Renukaradhya GJ, Narasimhan B, Mallapragada SK. Respiratory nanoparticle-based vaccines and challenges associated with animal models and translation. *J Control Release* 2015;219:622–31.
- [37] Torres MP, Wilson-Welder JH, Lopac SK, Phanse Y, Carrillo-Conde B, Ramer-Tait AE, et al. Poly(hydroxybutyrate) microparticles enhance dendritic cell antigen presentation and activation. *Acta Biomater* 2011;7:2857–64.
- [38] Huntimer LM, Ross KA, Darling RJ, Winterwood NE, Boggiatto P, Narasimhan B, et al. Poly(hydroxybutyrate) nanovaccine platform enhances antigen-specific cytotoxic T cell responses. *Technology* 2014;2:171–5.
- [39] Joshi VB, Geary SM, Carrillo-Conde BR, Narasimhan B, Salem AK. Characterizing the antitumor response in mice treated with antigen-loaded poly(hydroxybutyrate) microparticles. *Acta Biomater* 2013;9:5583–9.
- [40] Huntimer L, Wilson-Welder JH, Ross K, Carrillo-Conde B, Pruisner L, Wang C, et al. Single immunization with a suboptimal antigen dose encapsulated into poly(hydroxybutyrate) microparticles promotes high titer and avid antibody responses. *J Biomed Mater Res B Appl Biomater* 2013;101:91–8.
- [41] Ulery BD, Kumar D, Ramer-Tait AE, Metzger DW, Wannemuehler MJ, Narasimhan B. Design of a protective single-dose intranasal nanoparticle-based vaccine platform for respiratory infectious diseases. *PLoS ONE* 2011;6:e17642.
- [42] Foged C, Brodin B, Frokjaer S, Sundblad A. Particle size and surface charge affect particle uptake by human dendritic cells in an in vitro model. *Int J Pharm* 2005;298:315–22.
- [43] Chithrani BD, Ghazani AA, Chan WC. Determining the size and shape dependence of gold nanoparticle uptake into mammalian cells. *Nano Lett* 2006;6:662–8.
- [44] Brenza TM, Petersen LK, Zhang Y, Huntimer LM, Ramer-Tait AE, Hostetter JM, et al. Pulmonary biodistribution and cellular uptake of intranasally administered monodisperse particles. *Pharm Res* 2015;32:1368–82.
- [45] Petersen LK, Huntimer L, Walz K, Ramer-Tait A, Wannemuehler MJ, Narasimhan B. Combinatorial evaluation of in vivo distribution of poly(hydroxybutyrate) particle-based platforms for vaccine delivery. *Int J Nanomed* 2013;8:2213–25.